



**Fermi National Accelerator Laboratory**

# **Helical solenoid studies for the muon cooling channel**

**Mauricio Lopes**

**02/12/2008**

# 1 Introduction

This work summarizes the results of the design of the four sections for the muon cooling channel using helical solenoids [1].

The helical solenoid and its geometric parameters can be seen in Figure 1. The geometry was designed in order to achieve the target values for solenoid, helical dipole and quadrupole fields given some constrains such as period ( $\lambda$ ) and orbit radius ( $a$ )

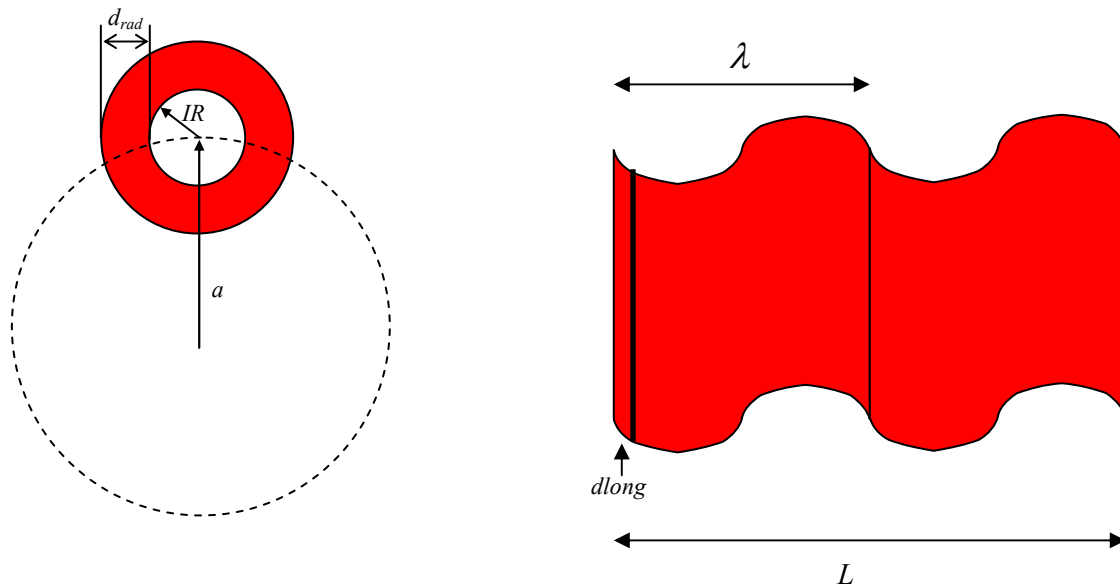


**Figure 1 - Helical solenoid design parameters**

A sensitivity study was done in order to evaluate the changes in the helical dipole and quadrupole as function of one of the design parameters.

For prototype purposes, short models of these magnets were simulated. The shot versions are one period long. Another version of only four coils was also simulated.

The forces (radial and longitudinal) distributions in a ring were calculated in order to feed future mechanical analysis simulations.

A short section is dedicated to the discussion of a Hybrid model for the 4<sup>th</sup> section made of HTS and Nb<sub>3</sub>Sn.

## 2 Definitions and notations

In this document it was considered two possible SC materials: Nb<sub>3</sub>Sn and HTS.

### *Characteristics for Nb<sub>3</sub>Sn*

It was considered for the packing factor of this SC the following:

$$PF = PF_{strand} * PF_{cable} * PF_{coil} = 0.5 * 0.85 * 0.9 = 0.38$$

Summers parameterization of the critical surface:

$$B_{c2}(0) = 27 \text{ T}, T_c(0) = 18 \text{ K}, J_c(12 \text{ T}, 4.2 \text{ K}) = 3 \text{ kA/mm}^2$$

### *Characteristics for HTS*

The HTS material considered in this work was the Bi-2212 and follows the measurements presented in [2]. In general, the critical surface already takes into account the engineering current density.

### *Field notation*

Solenoidal field is the **B<sub>z</sub>** field component.

Dipolar field (**B**) is the tangential field component shown in Figure 2.

Gradient (**G**) is the radial derivative (**dr**) of the dipolar field (**B**) (see Figure 2).

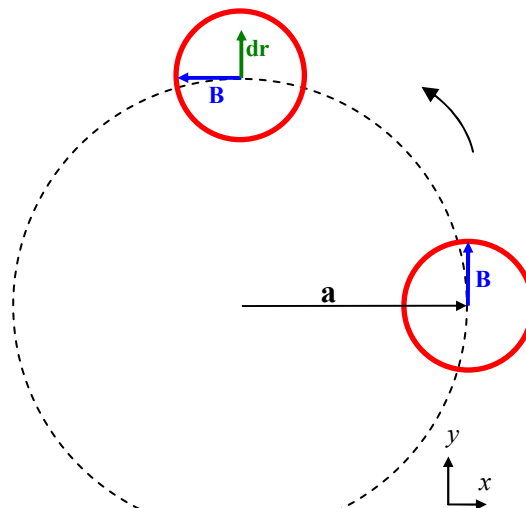


Figure 2 - Field notations

### 3 Simulation

Table 1 summarizes the design parameters and the performance of the four helical solenoids for the different sections. The geometrical parameters were optimized in order to match solenoidal field as well as the helical dipole and quadrupole. The three first sections are intended to be made of Nb<sub>3</sub>Sn. The fourth section is intended to be made of HTS.

Figure 3 shows the operation points for the Nb<sub>3</sub>Sn sections (with its critical surface) and Figure 4 shows the operation point for the HTS sections (with its critical surface). In all the cases it was aimed a safety margin around of 100%. The third section it's only achievable this safety margin using Nb<sub>3</sub>Sn. Therefore, the same section was modeled using HTS.

It is not possible to match the values for the helical dipole and quadrupole simultaneously. Therefore, the values presented in Table 1 are the optimum ones. In the next section it is presented a discussion about the influence of the design parameters in the fields.

			1st - Nb <sub>3</sub> Sn		2nd - Nb <sub>3</sub> Sn		3rd - Nb <sub>3</sub> Sn		3rd - HTS		4th - HTS	
			target	simulated	target	simulated	target	simulated	target	simulated	target	simulated
Total length	L	m	50	5	40	5	30	5	30	5	50	5
Period	$\lambda$	m	1.000	1.000	0.800	0.800	0.600	0.600	0.600	0.600	0.400	0.400
Orbit radius	a	m	0.160	0.160	0.130	0.130	0.095	0.095	0.095	0.095	0.060	0.060
Internal radius	IR	m	-	0.230	-	0.150	-	0.100	-	0.093	-	0.05
Coil radial thickness	drad	mm	-	50	-	110	-	150	-	100	-	150
Coil longitudinal thickness	dlong	mm	-	20	-	20	-	30	-	30	-	30
Numer coils per period	NCper		-	45	-	36	-	18	-	18	-	12
Solenoidal field	Bz	T	-6.95	-6.95	-8.69	-8.69	-11.60	-11.60	-11.60	-11.60	-17.30	-17.30
Helical dipole field	B	T	1.62	1.54	2.03	1.95	2.71	2.19	2.71	2.70	4.06	2.87
Helical field gradient	G	T/m	-0.70	-1.07	-1.10	-1.83	-2.00	-2.01	-2.00	-3.98	-4.50	-3.53
Maximum field in the coil at operational point		T	0	9.53	0	11.10	0	13.94	0	14.26	0	19.54
Operational current density		A/mm <sup>2</sup>	0	453.14	0	258.41	0	244.32	0	126.55	0	118.02
SSL Field		T	0	17.44	0	19	0	19.90	0	28.02	0	35.93
SSL Current density		A/mm <sup>2</sup>	0	829.66	0	449	0	348.71	0	248.77	0	217.04
Safety margin		%	-	83	-	74	-	43	-	97	-	84
Maximum radial force		MN	-	1.44	-	2.10	-	5.11	-	5.41	-	10.38
Maximum longitudinal force		MN	-	0.27	-	0.41	-	0.83	-	0.98	-	1.43

Table 1 - Design and performance of the different sections

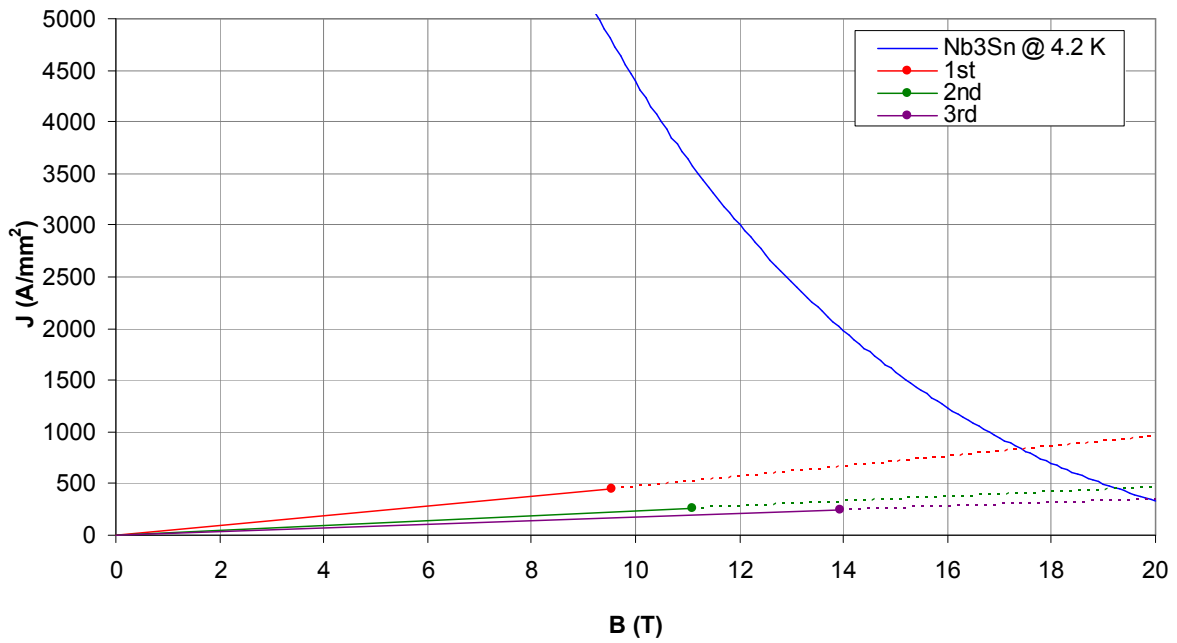


Figure 3 - Operation points for sections 1 to 3 made with Nb<sub>3</sub>Sn

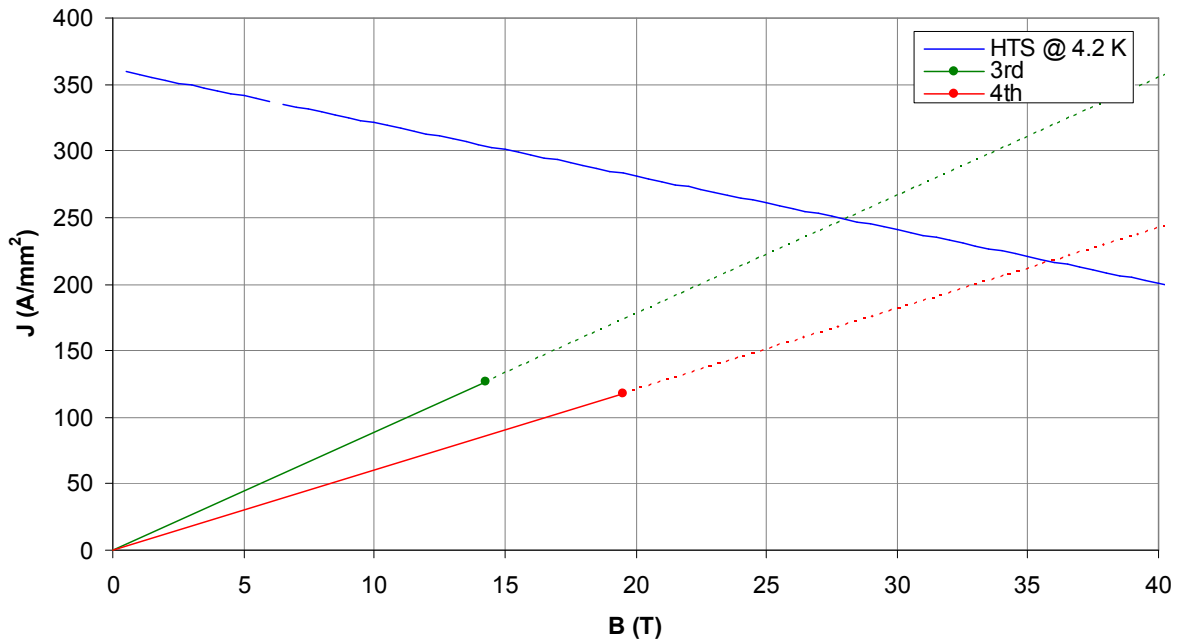


Figure 4 - Operation point for section 4 made with HTS

Figures 5 and 6 show the aspect of the first and fourth sections, respectively.

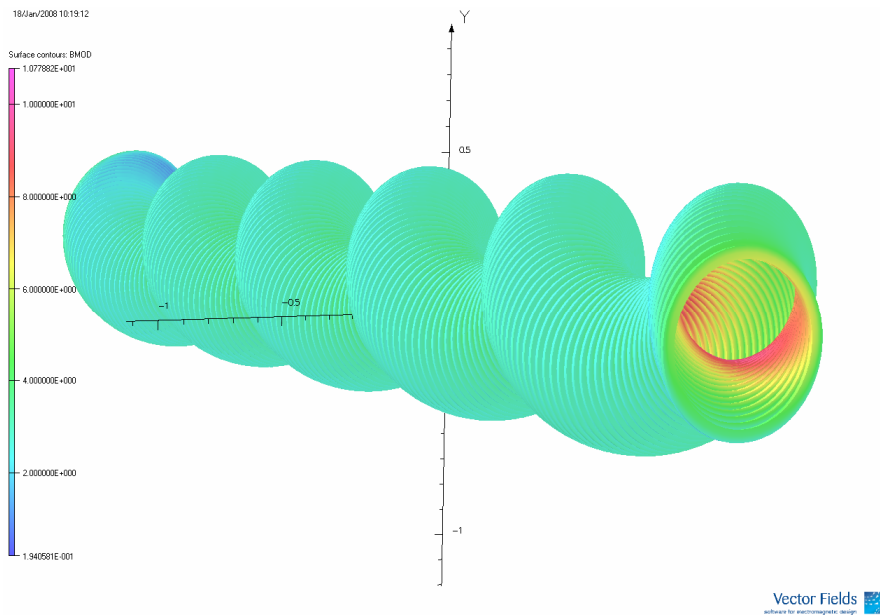


Figure 5 - 1<sup>st</sup> section

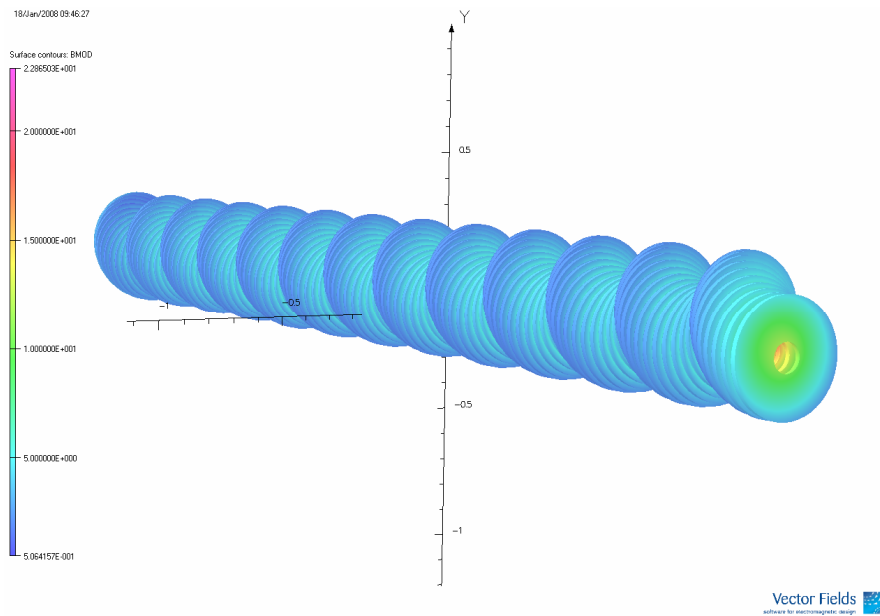
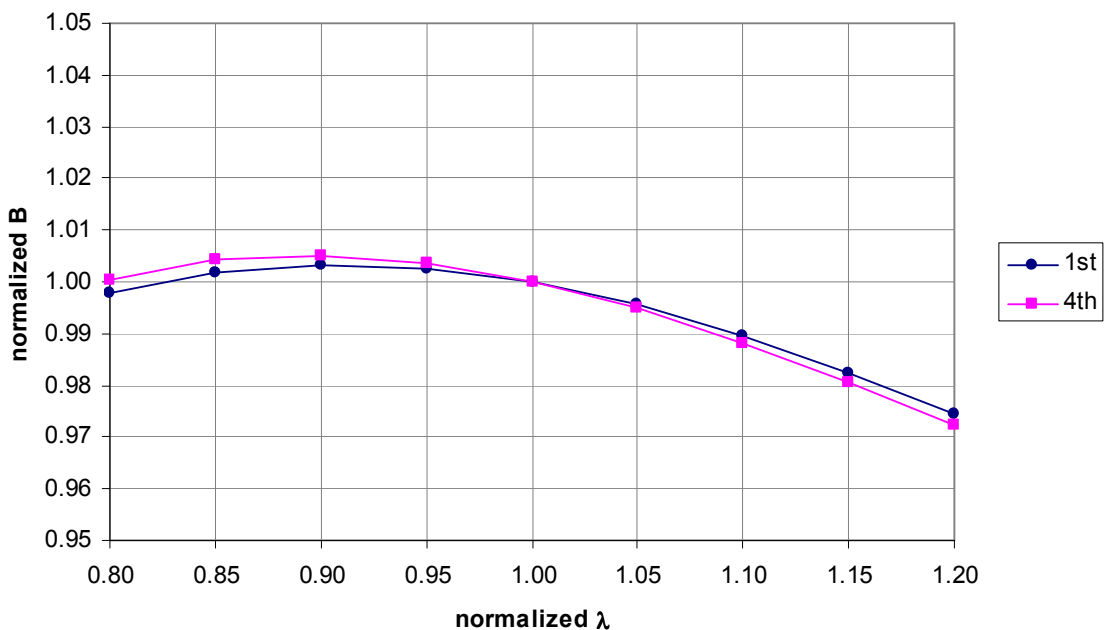


Figure 6 - 4<sup>th</sup> section

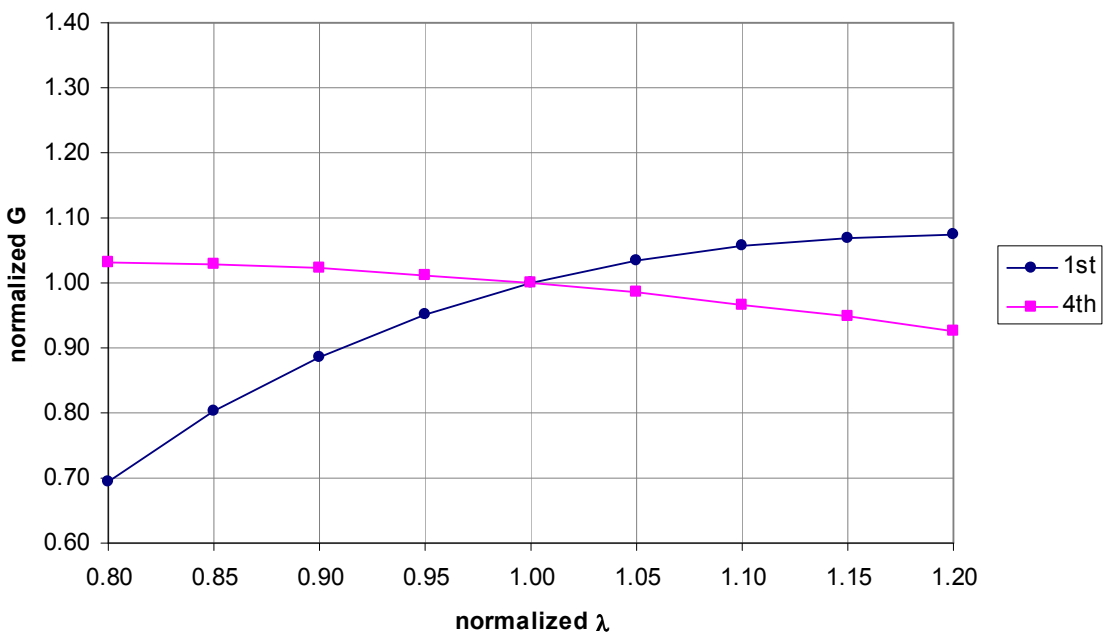
## 4 Parametric study

As can be concluded from the previous section, it is difficult to match all the three specified fields. However the field could be in some level tuned to match the helical dipole or quadrupole depending on the demand. In Figures 7-9 we present the relative changes in the dipole ( $B$ ) and gradient ( $G$ ) due to relative changes in one of the parameters ( $\lambda$ ,  $IR$ ,  $d_{rad}$ ) for the first and fourth sections. The solenoidal field was kept constant.

As can be seen, changes in the period ( $\lambda$ ) do not affect the helical dipole but affects the gradient. Changes in the internal radius ( $IR$ ) affect the dipole and the gradient fields. The changes in the radial coil thickness can be understood as an additional change in the “effective” internal radius. That is the reason for the big differences between the first and fourth sections: the coil thickness for the first section is relatively small compared to the other dimensions (internal radius, orbit radius).

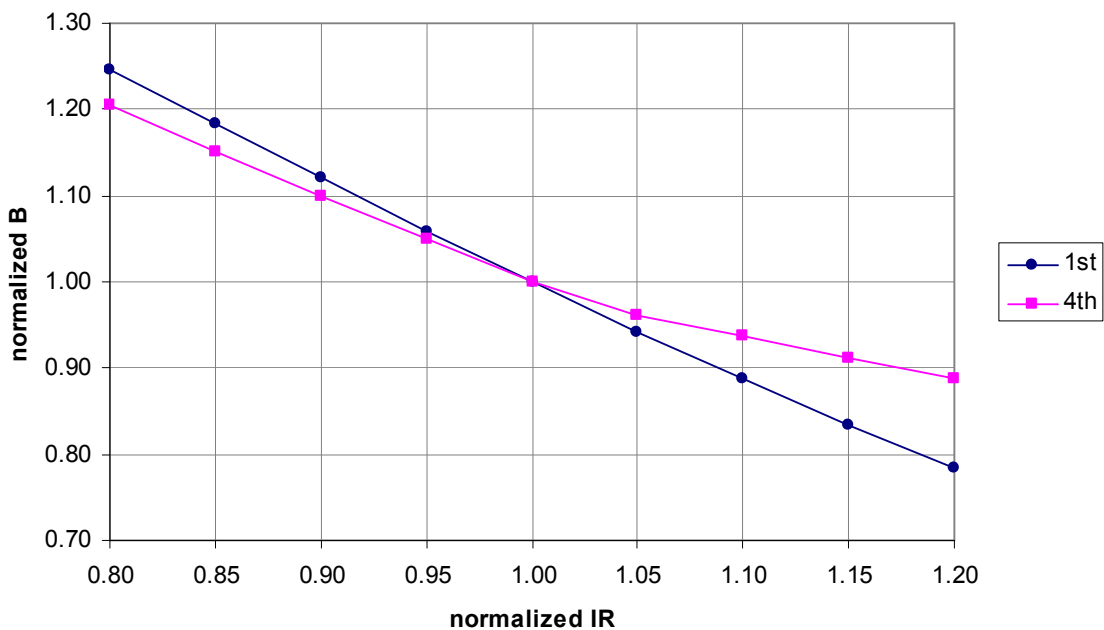


(a)

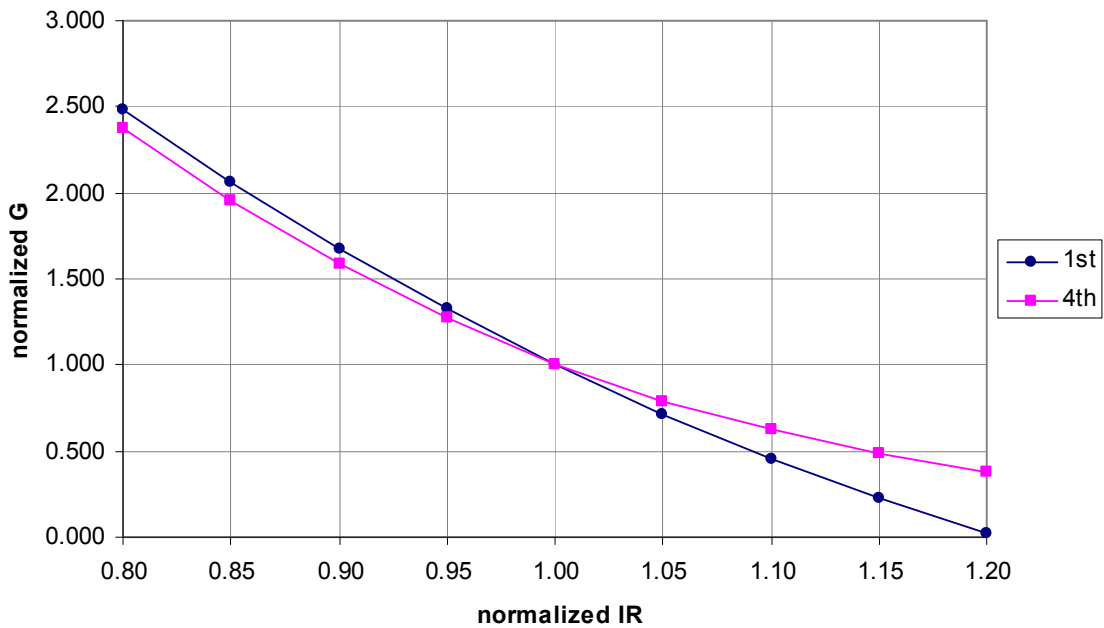


(b)

Figure 7 - Changes in the (a) dipole and (b) quadrupole as function of  $\lambda$

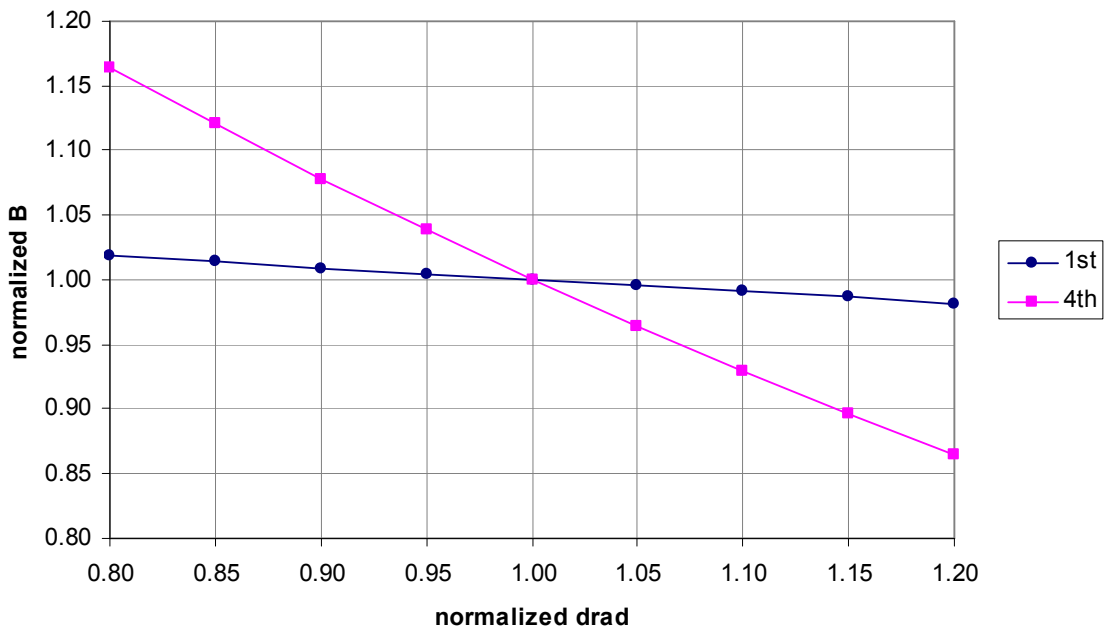


(a)

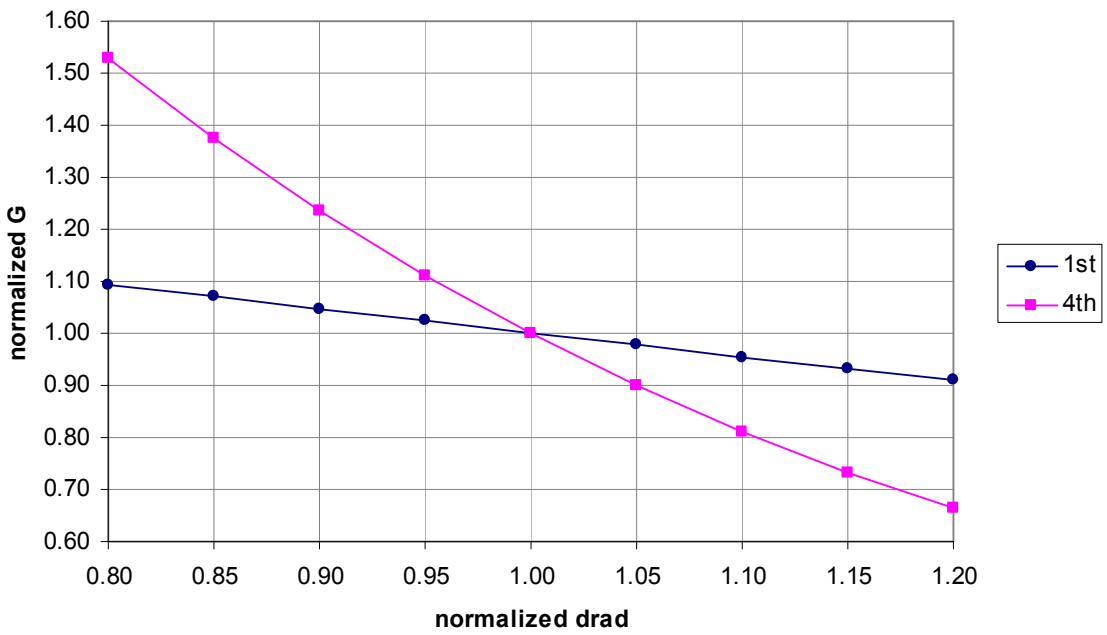


(b)

Figure 8 - Changes in the (a) dipole and (b) quadrupole as function of *IR*



(a)



(b)

Figure 9 - Changes in the (a) dipole and (b) quadrupole as function of *drad*

## 5 Short model

For the prototype purposes is important to simulated and analyze what would be the changes in the fields. For that it was kept the same design parameters but the length was set to only one helical period. Figure 10 shows an example for the short model.

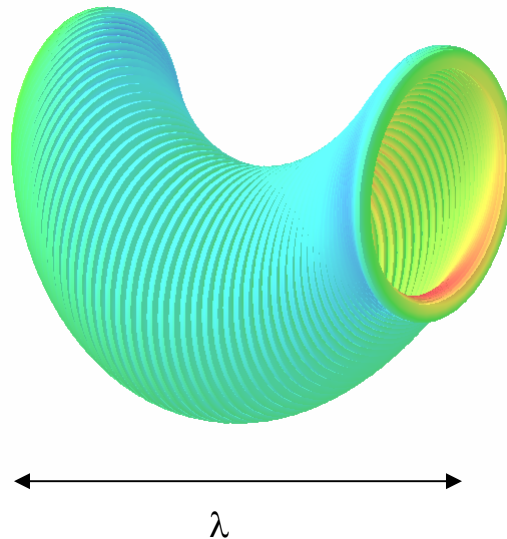


Figure 10 - Short model

Table 2 shows the performance parameters for the short models. The reduction in the solenoidal field is about of 15%.

			1st - Nb <sub>3</sub> Sn	2nd - Nb <sub>3</sub> Sn	3rd - Nb <sub>3</sub> Sn	3rd - HTS	4th - HTS
Total length	L	m	1.000	0.800	0.600	0.600	0.400
Period	λ	m	1.000	0.800	0.600	0.600	0.400
Orbit radius	a	m	0.160	0.130	0.095	0.095	0.060
Internal radius	IR	m	0.230	0.150	0.1	0.093	0.05
Coil radial thickness	drad	mm	50	110	150	100	150
Coil longitudinal thickness	dlong	mm	20	20	30	30	30
Numer coils per period	NCper		45	36	18	18	12
Solenoidal field	Bz	T	-6.29	-7.84	-10.19	-10.59	-14.94
Helical dipole field	B	T	1.62	2.05	2.35	2.82	3.10
Helical field gradient	G	T/m	-1.20	-2.04	-2.35	-4.30	-4.15
Maximum field in the coil at operational point		T	8.76	10.11	12.4	13.1	17.0
Operational current density		A/mm <sup>2</sup>	453.14	258.41	244.32	126.55	118.02
SSL Field			17.20	19.05	19.6	26.5	33.0
SSL Current density			890.15	487.12	387.80	255.05	228.96
Safety margin			96	89	59	102	94
Maximum radial force		MN	1.32	1.92	4.53	4.98	9.02
Maximum longitudinal force		MN	0.28	0.43	0.88	1.03	1.55
Storage energy	U	MJ	3.66	2.69	2.29	1.74	1.54

Table 2 - Design and performance of the different sections for the short models

## 6 Force distribution

The Lorentz forces in the central coil were calculated and they could be divided in two categories: radial forces (which is shown in Figure 11) and longitudinal forces (Figure 12). The calculations were done for the fourth section.

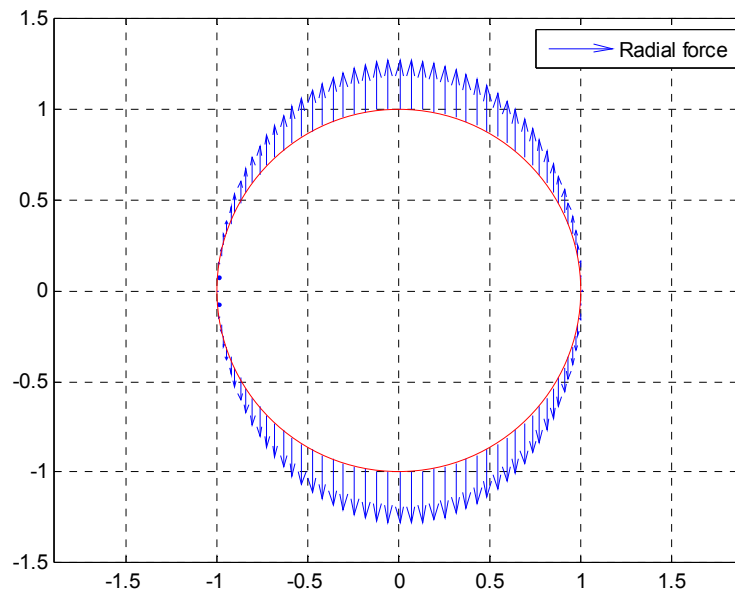


Figure 11 - Radial component of the force around the coil

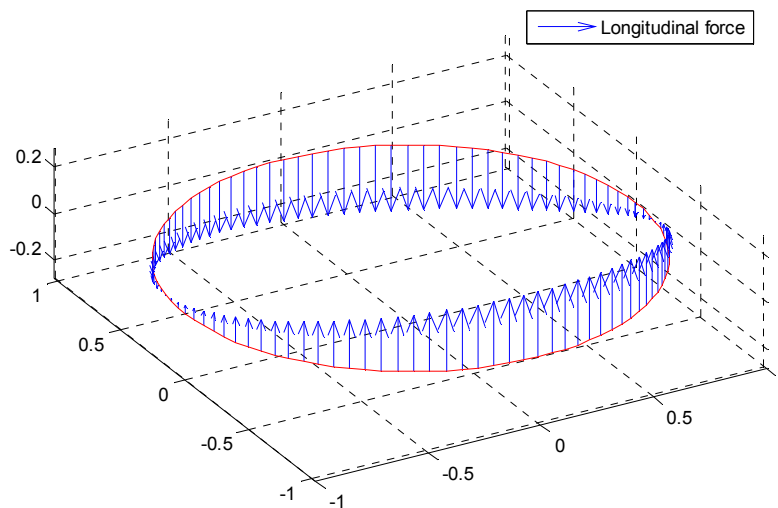


Figure 12 - Radial component of the force around the coil

Figure 13 show the force distribution around the coil. It can be noticed that the integral of the longitudinal component of the force is zero. However the coil will experience a torque

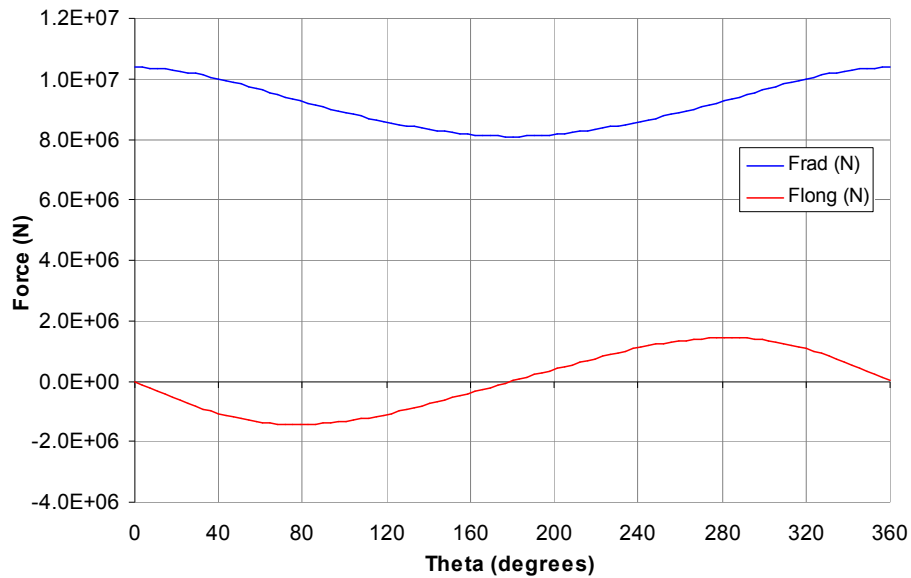


Figure 13 - Radial and longitudinal force distributions around the coil

## 7 Hybrid model for the 4<sup>th</sup> section

Given the fact that the peak field is located in the internal part of the coils, it was investigated the possibility of use a hybrid model composed of an internal coil made of HTS and an external coil made with Nb<sub>3</sub>Sn. Figure 14 shows an example of the hybrid model. Figure 15 show the operating points for the two parts of the coil.

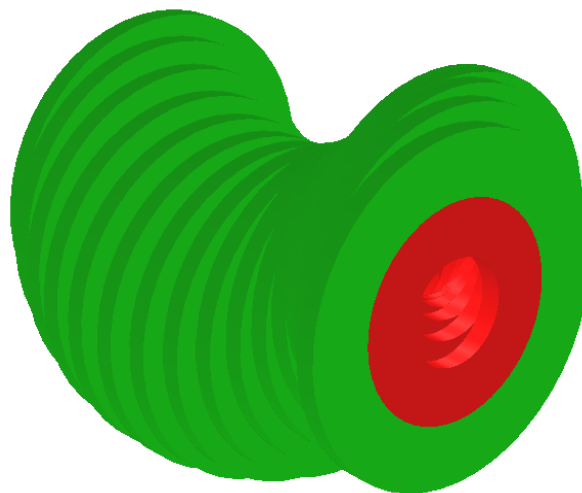


Figure 14 – Hybrid model

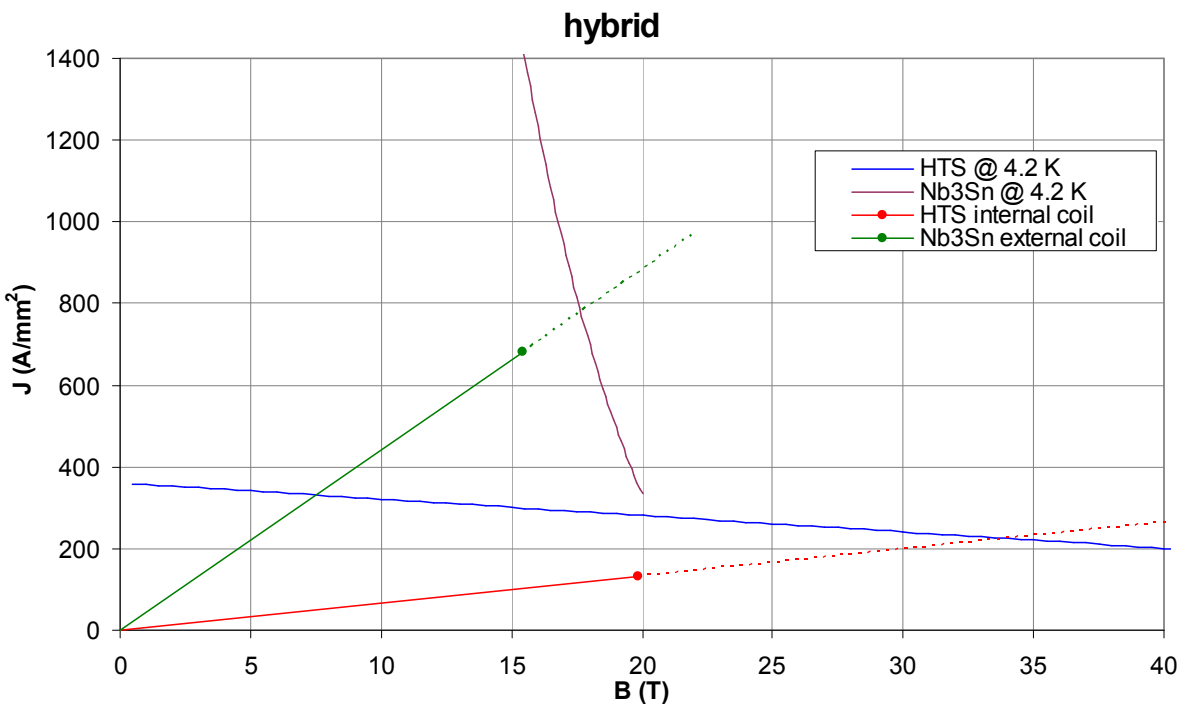


Figure 15 - Operation points for the hybrid model

Table 3 summarizes the design and performance parameters for the hybrid model.

			Target	Hybrid
Total length	L	m	50	5
Period	$\lambda$	m	0.400	0.400
Orbit radius	a	m	0.060	0.060
Internal radius	IR	m	-	0.0485
Internal coil radial thickness	d <sub>rad1</sub>	mm	-	52
External coil radial thickness	d <sub>rad2</sub>	mm	-	60
Coil longitudinal thickness	d <sub>long</sub>	mm	-	20
Numer coils per period	NC <sub>per</sub>		-	18
Solenoidal field	B <sub>z</sub>	T	-17.30	-17.30
Helical dipole field	B	T	4.06	3.90
Helical field gradient	G	T/m	-4.50	-6.42

Table 3 - Design and performance parameters for the hybrid model

## 8 Four-coil model

A four coil model of the fourth sections was done in order to evaluate the behavior of the fields in a first phase prototype development. Figure 16 shows the four coils model.

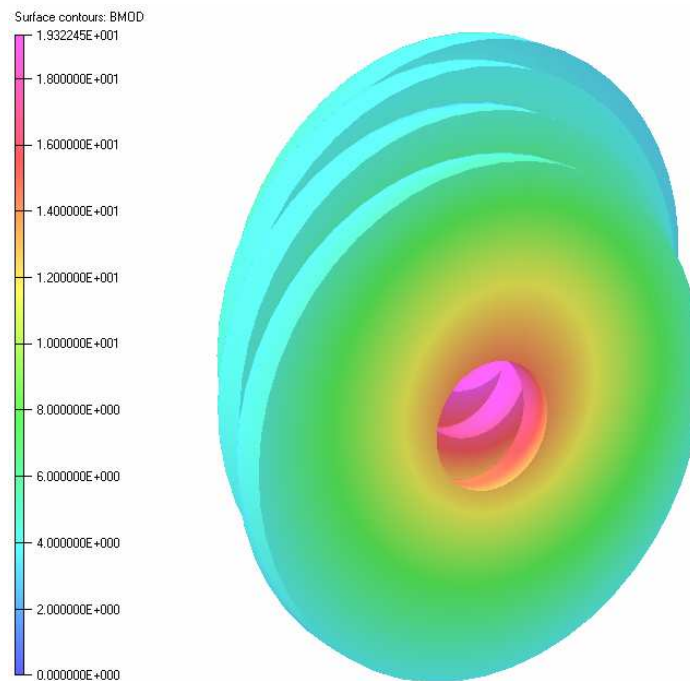


**Figure 16 - Four coils model for the fourth section**

			full length	4 coils
Total length	L	m	5.0	0.080
Period	$\lambda$	m	0.400	0.400
Orbit radius	a	m	0.060	0.060
Internal radius	IR	m	0.0485	0.0485
Coil radial thickness	drad	mm	145	145
Coil longitudinal thickness	dlong	mm	20	20
Numer coils per period	NCper		18	4
Solenoidal field	Bz	T	-17.30	-17.30
Helical dipole field	B	T	2.87	2.53
Helical field gradient	G	T/m	-3.53	6.12
Maximum field in the coil at operational point		T	19.54	19.16
Operational current density		A/mm <sup>2</sup>	118.02	211.52
SSL Field		T	35.93	24.00
SSL Current density		A/mm <sup>2</sup>	217.04	264.91
Safety margin		%	84	25
Maximum radial force	F	MN	10.38	18.23
Maximum longitudinal force	F	MN	1.43	1.84
Storage energy	U	MJ	-	0.94
Individual coil volume	V	m <sup>3</sup>	3.49E-03	3.49E-03

**Table 4 - Parameters for the four coils model**

## 9 Conclusions

The helical solenoids for the fourth cooling sections were design and evaluated. The main geometrical parameters were adjusted in order to match the helical dipole and quadrupole components. A sensitivity study of these parameters was also evaluated showing that the helical dipoles and quadrupoles could be fine adjusted but not the both together.

A short model of each section was simulated and the changes in the performance were shown. Basically there will be a reduction of the solenoidal field in about 15%.

The forces were evaluated and presented as radial and longitudinal components.

It was designed a hybrid model HTS - Nb<sub>3</sub>Sn for the fourth section.

A four coils model was also done for a first phase of prototyping.

The data contained in this report can be used to feedback the beam simulations in order to optimize the design parameters for this magnets.

## References

---

[1] K. Yonehara et al., EPAC06

[2] V. V. Kashikhin, E. Barzi, V. S. Kashikhin, M. Lamm, Y. Sadovskiy, and A. V. Zlobin, "Study of High Field Superconducting Solenoids for Muon Beam Cooling", Proceeding of Magnet technology conference 20, (2007)